The effect of carbohydrate binding modules and linkers on inhibitor binding to family 18 glycoside hydrolases

Kristine Bistrup Eide[a], *and Morten Sørlie*[a,]*

[a] Department of Chemistry, Biotechnology and Food Science, Norwegian University of Life Sciences, P.O. Box 5003, N-1432 Ås, Norway.

*Corresponding author: Tel: +47 64965902; fax: +47 64965901; e-mail: morten.sorlie@nmbu.no

ABSTRACT

Enzyme catalyzed hydrolysis of glycosidic bonds is undertaken by glycoside hydrolases (GHs) in nature. In addition to a catalytic domain (CD), GHs often have carbohydrate-binding modules (CBMs) attached to the CD through a linker. Allosamidin binding to full-length GH18 *Serratia marcescens* ChiB and the catalytic domain only yield equal changes in reaction free energy (ΔG_r^o = –38 kJ/mol), enthalpy (ΔH_r^o = 18 kJ/mol), and entropy ($-T\Delta S_r^o$ = –57 kJ/mol). Interestingly, the change in heat capacity ($\Delta C_{p,r}$) was 3-fold smaller for full-length vs. the CD alone (–263 vs. –695 J/K mol). Allosamidin binding to the full-length isoform and the CD alone of the GH18 human chitotriosidase yielded different ΔG_r^o (–46.9 vs. –38.9 kJ/mol) due to differences in ΔH_r^o (–58.2 vs. –50.2 kJ/mol), while $-T\Delta S_r^o$ and (11.3 vs. 11.3 kJ/mol) and $\Delta C_{p,r}$ (–531 vs. –602 kJ/mol) are similar. The results combined show that the nature of the linker region and CBM affect the thermodynamic signatures of active site ligand binding.

Keywords: Isothermal titration calorimetry; human chitinase, inhibition, enzyme mechanism.

1. Introduction

Enzymatic degradation of recalcitrant polysaccharides, such as cellulose and chitin, is of great biological and economical importance. In nature, enzymatic depolymerization of polysaccharides is accomplished by glycoside hydrolases (GHs). Chitin is degraded by enzymes called chitinases. These enzymes can be classified in two different GH families, family 18 and 19, depending on structure and mechanism (Henrissat and Davies, 1997). Family 19 chitinases are mainly found in plants and actinomycetes, while family 18 chitinases occur in many different organisms, including bacteria and human. The chitinolytic machinery of the Gram negative soil bacterium *Serratia marcescens* is one of the best known enzyme systems for the conversion of insoluble polysaccharides, consisting of four chitin-active enzymes; chitinase A (*Sm*ChiA), chitinase B (*Sm*ChiB), chitinase C (*Sm*ChiC), and chitin binding protein (CBP21), a surface-active lytic polysaccharide monooxygenase (LPMO) (Vaaje-Kolstad et al., 2013). The human genome codes for two active GH18 chitinases, acidic mammalian chitinase (AMCase) and human chitotriosidase (HCHT). HCHT, mainly found in circulation, is expressed and secreted in human macrophages, while AMCase is expressed in lung and stomach tissue (Boot et al., 2001, Zhu et al., 2004, Renkema et al., 1997). Both enzymes are believed to be a part of the innate immune system (van Eijk et al., 2007, Elias et al., 2005).

Common for all GHs are a catalytic domain (CD) hydrolyzing the glycosidic bonds between different carbohydrate moieties. In addition, GHs often have a supplementary carbohydrate-binding module (CBM) with carbohydrate-binding activity attached to the CD through a linker region (Boraston et al., 2004, Gilbert et al., 2013). Removal of CBMs often result in severely impaired binding to polymeric substrate (Watanabe et al., 1994, Varnai et al., 2013). HCHT occurs in two isoforms; one with a catalytic domain only (abbreviated HCHT39) and one variant with a family 14 CBM, consisting of 49 amino acids, attached C-terminally

through a 29-residue linker (abbreviated HCHT50) (Renkema et al., 1997, Lombard et al., 2014, Boraston et al., 2004). *Sm*ChiB occurs in a single isoform with a family 5 CBM attached through a C-terminal linker, about the same size (49 and 26 amino acids, respectively) as HCHT50 extending the positive subsite binding surface (van Aalten et al., 2000). Previous results suggest that the CBM of HCHT50 also extends positive subsite surfaces as observed in *Sm*ChiB (Stockinger et al., 2015). Still, *Sm*ChiB has a CBM with a flat surface more common for recalcitrant polysaccharide degradation, while the CBM of HCHT50 is associated with oligosaccharide binding (Boraston et al., 2004). Moreover, based on structural evidences available to date, bacterial GH18 chitinases appear to have their CBMs appended to the catalytic domain via a linker that is virtually fused against the surface of the catalytic domain, resulting in a compact, multi modular enzyme with an extended binding surface (Perrakis et al., 1994, van Aalten et al., 2000). In other enzyme families, such as families GH6 and GH7 active on cellulose, this linker region can be found as a solvent-exposed, intrinsically disordered peptide sequence (Payne et al., 2015, Wilson, 2004), preventing the acquiring of crystal structures. Interestingly, efforts to obtain a crystal structure of HCHT50 were fruitless until recently. The structure of the catalytic domain were solved in 2002 (Fusetti et al., 2002) and only through a combined cross-seeding and micro-seeding cycle approach were Fadel *et al*. able to obtain the crystal structure of the full-length enzyme (Fadel et al., 2016). Even so, the linker-region could not be modeled due to a lack of interpretable electron density due to the flexibility of this region. This suggests that the linker region of HCHT50 is less fused with the catalytic domain as seen for example *Sm*ChiB.

Ligand binding to an enzymes active site is accompanied by conformational changes in the protein-ligand complex. Since CBMs and their linker regions vary for selected GH18s, it is interesting to see if their presence affect the thermodynamics of active site binding. Previously, we have used isothermal titration calorimetry (ITC) to obtain the thermodynamic signature for

the allosamidin binding, a well-known family 18 chitinase inhibitor, to HCHT39 and *Sm*ChiB {Cederkvist, 2007 #79;Eide, 2013 #4}. In this work, we have investigated the binding of the same inhibitor to HCHT50 and *Sm*ChiB catalytic-domain only (*Sm*ChiB-CD) to assess the effect of the linkers and CBMs on GH18 active site ligand binding.

2. Experimental

2.1. Proteins and Chemicals

HCHT50 was overexpressed in HEK293-6E cells and purified as described elsewhere (Stockinger et al., 2015). For *Sm*ChiB-CD, mutagenesis of His_{10}-*Sm*ChiB-E144Q-G446 was performed using the QuickChange™ site directed mutagenesis from Stratagene (La Jolla, CA, USA), as described by the manufacturer. The primers used for the mutagenesis was designed as described by Westereng, 2002 (Westereng, 2002). The template in the mutagenesis was His_{10}-*Sm*ChiB-E144Q (Norberg et al., 2010). Then His_{10}-*Sm*ChiB-G446 (*Sm*ChiB-CD) was mutated by use of the following primers in the PCR reaction: 5'GGACATCGACTGGGAGTACCCGCAAGC'3 (forward) and 5'GCTTGCGGGTACTCCCAGTCGATGTCC'3 (reverse). To confirm the desired mutation, the mutated gene was sequenced using GATC Biotechs (Conctance, Germany) LIGHTrun Sequencing service. When desired mutation was confirmed, the gene was transformed into *Escherichia coli* BL21Star (DE3) cells (Life Technologies, Carlsbad, CA, USA). *Sm*ChiB-CD was further expressed and purified by the same method as described by Hamre et al., 2015 (Hamre et al., 2015). Enzyme purity was verified by SDS-PAGE and estimated to be above >95% in all cases. Protein concentration was determined by using the Bradford-method from Bio-Rad. Allosamidin was a kind gift from Professor Shohei Sakuda, University of Tokyo.

Allosamdin is isolated from *Streptomyces sp*. and the purity is controlled by ^{1}H NMR as described by Sakuda *et al*. (Sakuda et al., 1987). The structure of allosamidin has previously been verified by both NMR and crystallography (Sakuda et al., 1986). Buffers were made of potassium phosphate from Sigma-Aldrich (St. Louis, MO USA). The pH of final the solutions were controlled to be the desired one (pH 6.0) using glass electrode pH meter that was calibrated prior to use.

2.2. Isothermal titration calorimetry experiments

ITC experiments were performed with a VP-ITC system from Microcal, Inc (Northampton, MA) (Wiseman et al., 1989). Solutions were made by using Milli-Q watere and were thoroughly degassed prior to experiments to avoid air bubbles in the calorimeter. Standard ITC conditions were 250 μM of allosamidin in the syringe and 15 μM of HCHT50 or *Sm*ChiB-CD in the reaction cell in 20 mM potassium phosphate buffer of pH 6.0. Aliquots of 8 μL were injected into the reaction cell at 180 s intervals at temperatures of 20, 25, 30, and 37 °C with a stirring speed of 260 rpm. The titrations were normally complete after 22-27 injections. At least three independent titrations were performed for each binding reaction.

2.3 Analysis of calorimetric data

ITC data were collected automatically using the Microcal Origin v.7.0 software accompanying the VP-ITC system (Wiseman et al., 1989). Prior to further analysis, data were corrected for heat of dilution by subtracting the heat remaining after saturation of binding sites on the enzyme. Data were further fitted using a non-linear least-squares algorithm using a single-site binding model employed by the Origin software that accompanies the VP-ITC

system. All data from the binding reactions fitted well with the single-site binding model yielding the stoichiometry (n), equilibrium binding association constant (K_a), and the reaction enthalpy change ($\Delta H_r°$) of the reaction. The value of n was found to be between 0.9 and 1.1 for all reactions. The equilibrium binding dissociation constant (K_d), reaction free energy change ($\Delta G_r°$) and the reaction entropy change ($\Delta S_r°$) were calculated from the relationship described in Equation 1.

$$\Delta G_r° = -RT\ln K_a = RT\ln K_d = \Delta H_r° - T\Delta S_r° \quad (1)$$

Errors are reported as standard deviations of at least three experiments at each temperature. A description of how the entropic term is parameterized has been described in detail previously (Cederkvist et al., 2007, Zakariassen and Sørlie, 2007).

3. Results

3.1 Binding of allosamidin to HCHT50 and SmChiB-CD.

The binding of allosamidin to HCHT50 and *Sm*ChiB-CD (Fig. 1) at pH 6.0 (20 mM potassium phosphate buffer) at different temperatures (20-37 °C) was studied using ITC. Fig. 2 shows typical ITC thermograms and theoretical fits to the experimental data at t = 30 °C and pH 6.0. At this temperature, HCHT50 bind allosamidin with a K_d of = 0.008 ± 0.003 μM (ΔG_r° = –46.9 ± 0.5 kJ/mol, Table 1). The stoichiometry (n) was found to be 1.10 ± 0.03. The reaction was accompanied by an enthalpic change ($\Delta H_r°$) of –58.2 ± 0.8 kJ/mol and an entropic change of ($\Delta S_r°$) of –37 ± 3 J/K mol ($-T\Delta S_r°$ 11.3 ± 0.9 kJ/mol). The change in the heat of the reaction, as determined by Equation 2, was found to be –531 ± 13 J/K mol.

$$\Delta C^{o}_{p,r} = \left(\frac{\partial \Delta H^{o}_{r}}{\partial T} \right) \quad (2)$$

The binding of allosamidin to *Sm*ChiB-CD at t =30 °C gave a K_d of 0.18 ± 0.03μM (−39.1 ± 1.0 kJ/mol, Table 1). The stoichiometry (n) was found to be 0.95 ± 0.09. The reaction was accompanied by an enthalpic change ($\Delta H_r°$) of 18.4 ± 0.5 kJ/mol and an entropic change of ($\Delta S_r°$) of 189 ± 4 J/K mol ($-T\Delta S_r° = -57.5 \pm 1.1$ kJ/mol). The change in the heat of the reaction was determined to be −695 ± 40 J/K mol.

3.3 Parameterization of the Entropic Term.

The entropic term, $\Delta S_r°$, can be viewed as the sum of translational, solvation, and conformational entropic changes (Baker and Murphy, 1997) as seen in Equation 4.

$$\Delta S_r° = \Delta S°_{mix} + \Delta S°_{solv} + \Delta S°_{conf.} \quad (4)$$

By recognizing that the entropy of solvation is close to zero for proteins near T = 385 K, $\Delta C_{p,r}$ can be related to the solvation entropy change ($\Delta S°_{solv}$) of the binding reaction at t = 30 °C as described by Equation 5 (Baker and Murphy, 1997, Baldwin, 1986, Murphy et al., 1990).

$$\Delta S^{o}_{solv} = \Delta C^{o}_{p,r} \ln\left(\frac{303\,\mathrm{K}}{385\,\mathrm{K}} \right) \quad (5)$$

By using this relationship, a $\Delta S°_{solv}$ of 127 ± 3 J/K mol can be calculated representing −38.5 ± 0.9 kJ/mol ($-T\Delta S°_{solv}$) of the total free energy change of −46.9 kJ/mol for the binding reaction between HCHT50 and allosamidin (Table 1). For the binding reaction between *Sm*ChiB-CD

and allosamidin the following values were calculated: $\Delta S°_{solv}$ of 167 ± 7 J/K mol representing −50.5 ± 2.0 kJ/mol ($-T\Delta S°_{solv}$) of the total free energy change of −39.1 ± 1.0 kJ/mol.

Furthermore, the translational entropy change ($\Delta S°_{mix}$) of the reaction can be calculated as a 'cratic' term, a statistical correction that reflects mixing of solute and solvent molecules and the changes in translational / rotational degrees of freedom (Equation 6) (Baker and Murphy, 1997):

$$\Delta S^{o}_{mix} = R \ln\left(\frac{1}{55.5}\right) \qquad (6)$$

Using this approach, a $\Delta S°_{mix}$ of –33 J/K mol can be calculated corresponding to a $-T\Delta S°_{mix}$ of 10.0 kJ/mol for both HCHT50 and *Sm*ChiB-CD. This further allows for the calculation of the conformational entropy change ($\Delta S°_{conf}$) described by Equation 3. For HCHT50 $\Delta S°_{conf}$ was calculated to be 131 ± 4 J/K mol, corresponding to a $-T\Delta S°_{conf}$ of 39.8 ± 1.3 kJ/mol. For *Sm*ChiB-CD $\Delta S°_{conf}$ was found to be 56 ± 8 J/K mol corresponding to a $-T\Delta S°_{conf}$ of −17.0 ± 2.3 kJ/mol.

4. Discussion

CBMs are important for recognition and increasing GH concentration on the carbohydrate substrate (Boraston et al., 2004). Their significance is highlighted by the classification of CBMs into over 70 families in the Carbohydrate Active Enzymes database (CAZy) (www.cazy.org). The CBM5 of *Sm*ChiB has a flat surface commonly found for GHs, both chitinases and cellulases, that is supposed to accommodate and degrade crystalline polysaccharides while the CBM14 of HCHT50 is designed to bind oligosaccharides. One of the believed key roles of CBMs is to increase the concentration of enzyme on the substrate surfaces

(Varnai et al., 2014). Still, HCHT50 is markedly better at degrading a β-chitin substrate from crab shell than *Sm*ChiB with 100 % vs. 30 % substrate degradation efficiency, respectively (Hamre et al., 2014, Stockinger et al., 2015). Moreover, the presence of a CBM may also slow desorption from the substrate (Varnai et al., 2014), thus preventing new actions on the substrate, and it is often observed that substrate dissociation is the rate limiting step in polysaccharide degradation (Igarashi et al., 2011, Kurašin and Väljamäe, 2011, Kuusk et al., 2015). It may be that HCHT50 with its somewhat unusual CBM14 and a flexible linker that is sufficiently long enough to enable the location of this on both sides of catalytic domain is an overall architecture that enables efficient degradation of the recalcitrant polysaccharide chitin.

From this and previous works, we now have thermodynamic signatures for active-site ligand binding of two GH18s with different linker regions and CBMs and catalytic domains only (Table 1) (Eide et al., 2013, Cederkvist et al., 2007). Hence, the effect of linkers and CBMs on the overall binding thermodynamics can be assessed. The most important thermodynamic parameter is the free energy of binding (ΔG_r^o), as this summarizes the overall stability of the protein-ligand complex relative to the free species. Firstly, *Sm*ChiB and *Sm*ChiB-CD show equal affinity towards allosamidin with a ΔG_r^o of ~ – 39 kJ/mol. Moreover at t = 30 ºC, the unfavorable enthalpic (ΔH_r^o = ~18 kJ/mol) and the favorable entropic terms ($-T\Delta S_r^o$ = –57 kJ/mol) of the free energy of binding is equal. Interestingly, there are significant differences in the measured change of heat capacities ($\Delta C_{p,r}$) where there is a ~3-fold decrease in the change in heat capacity upon allosamidin binding upon removal of the CBM (−695 vs. −263 kJ/mol) (Fig. 3). A traditional interpretation has been that negative $\Delta C_{p,r}$ values are associated with changes in hydrophobic hydration and nonpolar accessible surface areas (Livingstone et al., 1991, Tomme et al., 1996) and that $\Delta C_{p,r}$ is linked to hydration of a system in general (Baker and Murphy, 1997, Murphy et al., 1990, Sturtevant, 1977, Baldwin, 1986). In line with this, it has been observed that $\Delta C_{p,r}$ is proportional with solvation entropy changes upon binding,

allowing the estimation of its value (Baldwin, 1986, Zolotnitsky et al., 2004, Livingstone et al., 1991). Allosamidin binding to *Sm*ChiB-CD is highly driven by desolvation of the protein and the ligand upon complexation, having a $-T\Delta S_{solv}^{o}$ of −50.5 kJ/mol, exceeding the total free energy of binding. Binding to the full length *Sm*ChiB is accompanied by a $-T\Delta S_{solv}^{o}$ of −21.0 kJ/mol constituting roughly half of the free energy of binding. Since the translational entropy change of allosamidin binding to both *Sm*ChiB and *Sm*ChiB-CD is of equal magnitude (and can be calculated), conformational entropy changes can be estimated. Here, it is interesting to observe that conformational entropy changes upon binding to the full length of *Sm*ChiB ($-T\Delta S_{conf}^{o}$ = −45.2 kJ/mol) is of equal magnitude as the free energy of binding while it is approximately half for *Sm*ChiB-CD ($-T\Delta S_{conf}^{o}$ = −17.0 kJ/mol).

Free energy of allosamidin binding to HCHT39 is equal to that of *Sm*ChiB and *Sm*ChiB-CD at t = 30 ºC, while it is 8 kJ/mol more favorable to HCHT50 due to an 8 kJ/mol more favorable enthalpic term (−58.2 vs. −50.2 kJ/mol) resulting in an equal, unfavorable entropic term for both isoforms ($-T\Delta S_{r}^{o}$ = 11.3 kJ/mol). Intriguingly, there are small differences in the measured change of heat capacities (−531 kJ/mol for HCHT50 vs. −602 kJ/mol for HCHT39, equal within experimental errors). This results in equally small differences in both solvation and conformation entropy changes since the reaction entropy change is the same for both isoforms.

It is highly interesting to observe that the presence of a CBM greatly affects the thermodynamic signatures of active site ligand binding for *Sm*ChiB while this is not the case for HCHT50. In biochemistry, the dissociation constant K_d, which is proportional to ΔG_r^{o}, is widely used to assess binding affinity. The introduction of ITC allows for simultaneous determination of the enthalpic and entropic terms in addition to K_d and ΔG_r^{o}. Still, as seen for *Sm*ChiB and *Sm*ChiB-CD, all these parameters are equal. Even so, the individual changes in heat capacities are markedly different. The parameterization of the entropic terms shows that

the linker and the CBM are important for the inducing of beneficial conformational changes upon binding. Conformational changes are indeed observed upon ligand binding in the crystal structure of *Sm*ChiB as well (van Aalten et al., 2001). Upon removal of the linker and the CBM, the beneficial conformational entropy changes decrease and the solvation entropy increase. Since the linker is clearly fused with the CD (Figure 1), it is not surprising to observe that its presence affects the thermodynamics upon binding. Similarly, it is not unexpected that the effect of the linker and the CBM for HCHT50 on the thermodynamics of binding is less pronounced. The lack of interpretable electron density of the linker region suggest this is intrinsically disordered (Fadel et al., 2016) as is common for i.e. family 6 and 7 cellulases (Payne et al., 2015).

Our results suggest that initial binding to the HCHT active site is not very influenced by the linker region nor by the CBM in contrast to what is observed for *Sm*ChiB. The flexibility of the linker may even allow the CBM of HCHT to move independently the catalytic domain on a crystalline substrate. The present study further confirm that HCHT50 shows atypical properties relative to bacterial enzymes (Eide et al., 2016)(Stockinger et al., 2015). In bacteria, several GHs are normally co-evolved to tackle the enzymatic degradation of the crystalline chitin structures while HCHT is the single systemic chitinase in humans. For this reason, it appears that HCHT harbors unique GH18 characteristics in line with its alleged physiological task of being a "complete" chitinolytic machinery by itself.

Acknowledgements

This work was supported by Grant 221576 from the Norwegian Research Council – Norway

Table 1.

Thermodynamic parameters (free energy change (ΔG), enthalpy change (ΔH), entropy change (ΔS), which in turn is divided in to conformational (conf), solvational (solv), and translational (mix) entropy, and change in heat capacity (ΔC_p)) for allosamidin binding to HCHT50, HCHT39, *Sm*ChiB, and *Sm*ChiB-CD at t = 30 °C and p = 1.01 Bar, as determined by isothermal titration calorimetry.

K_d[a]	ΔG_r°[b]	ΔH_r°[b]	$-T\Delta S_r^{\circ}$[b]	$-T\Delta S_{solv}^{\circ}$[b,c]	$-T\Delta S_{conf}^{\circ}$[b,d]	$-T\Delta S_{mix}^{\circ}$[b,e]	$\Delta C_{p,r}^{\circ}$[f,g]
HCHT50							
0.0083 ± 0.0028	−46.9 ± 0.5	−58.2 ± 0.8	11.3 ± 0.9	−38.5 ± 0.9	39.8 ± 1.3	10.0	−531 ± 13
HCHT39							
0.20 ± 0.03	−38.9 ± 0.4	−50.2 ± 1.2	11.3 ± 1.2	−43.7 ± 4.4	45.0 ± 4.2	10.0	−602 ± 63
*Sm*ChiB[h]							
0.16 ± 0.04	−38.0 ± 1.0	18.5 ± 0.9	−56.5 ± 1.7	−21.0 ± 1.1	−45.2 ± 2.0	10.0	−263 ± 16
*Sm*ChiB-CD							
0.18 ± 0.03	−39.1 ± 1.0	18.4 ± 0.5	−57.5 ± 1.1	−50.5 ± 2.0	−17.0 ± 2.3	10.0	−695 ± 40

[a] μM; [b] (kJ/mol); [c] $\Delta S_{solv}^{o} = \Delta C_p \ln(T_{303\ K}/T_{385\ K})$ (Baker and Murphy, 1997, Baldwin, 1986, Murphy et al., 1990); [d] derived using $\Delta S_r^{\circ} = \Delta S_{solv}^{o} + \Delta S_{mix}^{o} + \Delta S_{conf}^{o}$; [e] $\Delta S_{mix}^{o} = R\ln(1/55.5) = -33$ J/K mol ("cratic" term) [24]; [f] (J/K mol); [g] these data are derived from the temperature dependence of ΔH_r°; [h] from Cederkvist *et al*. (Cederkvist et al., 2007).

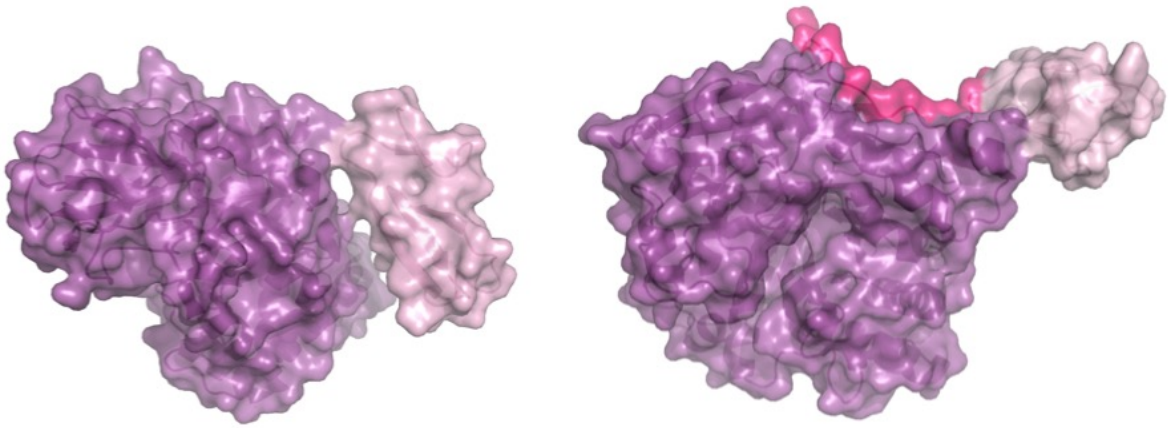

Fig. 1. Structure of HCHT50 (pdb code 5hbf) (left), and *Sm*ChiB (pdb code 1e6r (van Aalten et al., 2001)) (right). The catalytic domains are colored in magenta while the carbohydrate-

binding modules are colored in pink. For *Sm*ChiB, the linker region is colored in hotpink. This region of HCHT50 could not be modeled due to a lack of interpretable electron density due to the flexibility of this region.

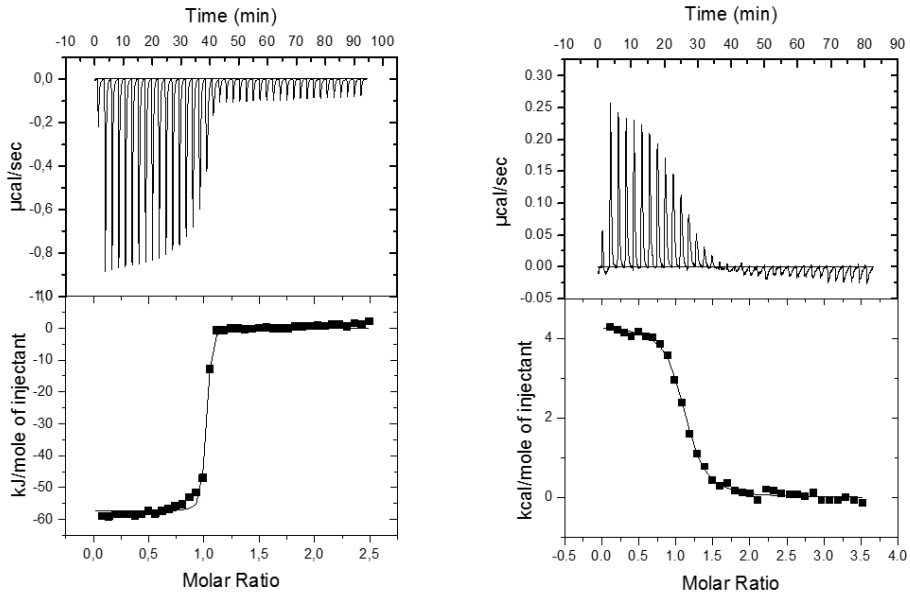

Fig. 2. Thermograms (upper panels) and binding isotherms with theoretical fits (lower panels) for the titration of allosamidin to HCHT50 (left) and *Sm*ChiB-CD (right) at t = 30 °C in 20 mM potassium phosphate buffer at pH 6.0.

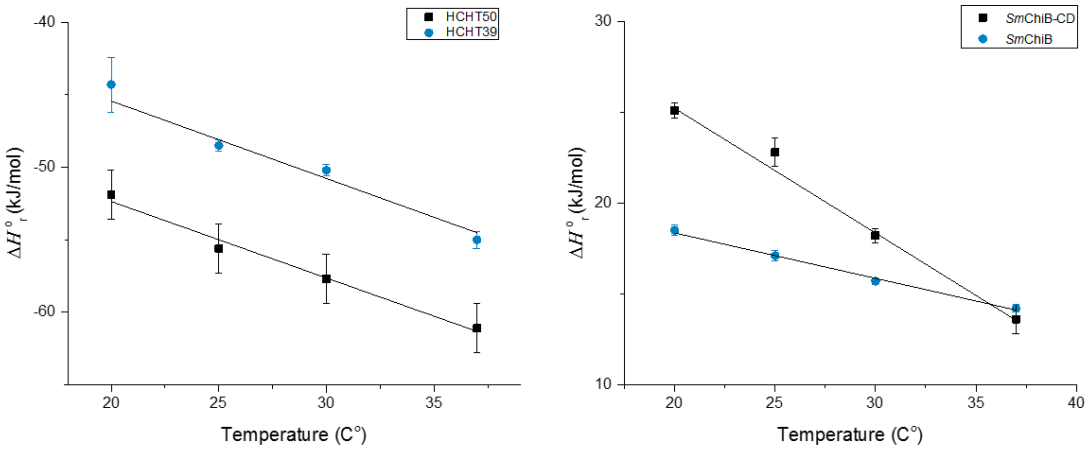

Fig 3. The plot of $\Delta H_r°$ vs. temperature yields the change of heat capacity ($\Delta C_{p,r}$) as the slope. The left panel gives the temperature dependence of allosamidin binding to HCHT39 and HCHT50 at pH 6.0. The $\Delta C_{p,r}$ value for HCHT50 and HCHT39 are −531 ± 13 J/K mol and −602 ± 63 J/K mol, respectively. The right panel gives the temperature dependence of allosamidin binding to *Sm*ChiB and *Sm*ChiB-CD at pH 6.0. The $\Delta C_{p,r}$ value for *Sm*ChiB and *Sm*ChiB-CD are −263 ± 16 J/K mol and −695 ± 40 J/K mol, respectively.

References

BABAN, J., FJELD, S., SAKUDA, S., EIJSINK, V. G. H. & SØRLIE, M. 2010. The Roles of Three Serratia marcescens Chitinases in Chitin Conversion Are Reflected in Different Thermodynamic Signatures of Allosamidin Binding. *J.Phys.Chem.B,* 114**,** 6144-6149.

BAKER, B. M. & MURPHY, K. P. 1997. Dissecting the energetics of a protein-protein interaction: the binding of ovomucoid third domain to elastase. *J.Mol.Biol.,* 268**,** 557-569.

BALDWIN, R. L. 1986. Temperature dependence of the hydrophobic interaction in protein folding. *Proc.Natl.Acad.Sci.USA,* 83**,** 8069-8072.

BOOT, R. G., BLOMMAART, E. F. C., SWART, E., GHAUHARALI-VAN DER VLUGT, K., BIJL, N., MOE, C., PLACE, A. & AERTS, J. M. F. G. 2001. Identification of a novel acidic mammalian chitinase distinct from chitotriosidase. *J. Biol. Chem.,* 276**,** 6770-6778.

BORASTON, A. B., BOLAM, D. N., GILBERT, H. J. & DAVIES, G. J. 2004. Carbohydrate-binding modules: fine-tuning polysaccharide recognition. *Biochem. J.,* 382**,** 769-781.

CEDERKVIST, F. H., SAUA, S. F., KARLSEN, V., SAKUDA, S., EIJSINK, V. G. H. & SØRLIE, M. 2007. Thermodynamic Analysis of Allosamidin Binding to a Family 18 Chitinase. *Biochemistry,* 46**,** 12347-12354.

EIDE, K. B., LUNDMARK, S. T., SAKUDA, S. & SØRLIE, M. 2013. Thermodynamic analysis of allosamidin binding to the Human chitotriosidase. *Thermochim. Acta,* 565**,** 146-150.

EIDE, K. B., NORBERG, A. L., HEGGSET, E. B., LINDBOM, A. R., VÅRUM, K. M., EIJSINK, V. G. H. & SØRLIE, M. 2012. The Action of the Human Chitriosidase on Chitosan. *Biochemistry,* 51**,** 487-495.

EIDE, K. B., STOCKINGER, L. W., LEWIN, A. S., TONDERVIK, A., EIJSINK, V. G. H. & SORLIE, M. 2016. The role of active site aromatic residues in substrate degradation by the human chitotriosidase. *Biochim. Biophys. Acta-Prot. Proteom.,* 1864**,** 242-247.

ELIAS, J. A., HOMER, R. J., HAMID, Q. & LEE, C. G. 2005. Chitinases and chitinase-like proteins in TH2 inflammation and asthma. *J. Allergy Clin. Immunol.,* 116**,** 497-500.

FADEL, F., ZHAO, Y. G., COUSIDO-SIAH, A., RUIZ, F. X., MITSCHLER, A. & PODJARNY, A. 2016. X-Ray Crystal Structure of the Full Length Human Chitotriosidase (CHIT1) Reveals Features of Its Chitin Binding Domain. *Plos One,* 11**,** 15.

FUSETTI, F., VON MOELLER, H., HOUSTON, D., ROZEBOOM, H. J., DIJKSTRA, B. W., BOOT, R. G., AERTS, J. M. F. G. & VAN AALTEN, D. M. F. 2002. Structure of Human Chitotriosidase. Implications for Specific Inhibitor Design and Function of mMammalian Chitinase-Like Lectins. *J. Biol. Chem.,* 277**,** 25537-25544.

GILBERT, H. J., KNOX, J. P. & BORASTON, A. B. 2013. Advances in understanding the molecular basis of plant cell wall polysaccharide recognition by carbohydrate-binding modules. *Curr Opin Struct Biol,* 23**,** 669-77.

HAMRE, A. G., JANA, S., HOLEN, M. M., MATHIESEN, G., VÄLJAMÄE, P., PAYNE, C. M. & SØRLIE, M. 2015. Thermodynamic Relationships with Processivity in Serratia marcescens Family 18 Chitinases. *The Journal of Physical Chemistry B,* 119**,** 9601-9613.

HAMRE, A. G., LORENTZEN, S. B., VALJAMAE, P. & SORLIE, M. 2014. Enzyme processivity changes with the extent of recalcitrant polysaccharide degradation. *FEBS Lett.,* 588**,** 4620-4624.

HENRISSAT, B. & DAVIES, G. J. 1997. Structural and sequence-based classification of glycoside hydrolases. *Curr. Opin. Struct. Biol.,* 7**,** 637-644.

IGARASHI, K., UCHIHASHI, T., KOIVULA, A., WADA, M., KIMURA, S., OKAMOTO, T., PENTTILÄ, M., ANDO, T. & SAMEJIMA, M. 2011. Traffic Jams Reduce Hydrolytic Efficiency of Cellulase on Cellulose Surface. *Science,* 333**,** 1279-1282.

KURAŠIN, M. & VÄLJAMÄE, P. 2011. Processivity of cellobiohydrolases is limited by the substrate. *J. Biol. Chem.,* 286**,** 169-177.

KUUSK, S., SØRLIE, M. & VALJAMAE, P. 2015. The Predominant Molecular State of Bound Enzyme Determines the Strength and Type of Product Inhibition in the Hydrolysis of Recalcitrant Polysaccharides by Processive Enzymes. *J. Biol. Chem.,* 290**,** 11678-11691.

LIVINGSTONE, J. R., SPOLAR, R. S. & RECORD, M. T. 1991. Contribution to the thermodynamics of protein folding from the reduction in water-accessible nonpolar surface area. *Biochemistry,* 30**,** 4237-4244.

LOMBARD, V., GOLACONDA RAMULU, H., DRULA, E., COUTINHO, P. M. & HENRISSAT, B. 2014. The carbohydrate-active enzymes database (CAZy) in 2013. *Nucleic Acids Research,* 42**,** D490-D495.

MURPHY, K. P., PRIVALOV, P. L. & GILL, S. J. 1990. Common features of protein unfolding and dissolution of hydrophobic compounds. *Science,* 247**,** 559-561.

NORBERG, A. L., KARLSEN, V., HOELL, I. A., BAKKE, I., EIJSINK, V. G. H. & SØRLIE, M. 2010. Determination of substrate binding energies in individual subsites of a family 18 chitinase. *FEBS Lett.,* 584**,** 4581-4585.

PAYNE, C. M., KNOTT, B. C., MAYES, H. B., HANSSON, H., HIMMEL, M. E., SANDGREN, M., STAHLBERG, J. & BECKHAM, G. T. 2015. Fungal Cellulases. *Chem. Rev.,* 115**,** 1308-1448.

PERRAKIS, A., TEWS, I., DAUTER, Z., OPPENHEIM, A. B., CHET, I., WILSON, K. S. & VORGIAS, C. E. 1994. Crystal structure of a bacterial chitinase at 2.3 A resolution. *Structure.,* 2**,** 1169-1180.

RENKEMA, G. H., BOOT, R. G., STRIJLAND, A., DONKER-KOOPMAN, W. E., VAN DEN BERG, M., MUIJSERS, A. O. & AERTS, J. M. F. G. 1997. Synthesis, sorting, and processing into distinct isoforms of human macrophage chitotriosidase. *Eur. J. Biochem.,* 244**,** 279-285.

SAKUDA, S., ISOGAI, A., MATSUMOTO, S. & SUZUKI, A. 1987. Search for microbial insect growth regulators. II. Allosamidin, a novel insect chitinase inhibitor. *J Antibiot.(Tokyo),* 40**,** 296-300.

SAKUDA, S., ISOGAI, A., MATSUMOTO, S., SUZUKI, A. & KOSEKI, K. 1986. The structure of allosamidin, a novel insect chitinase inhibitor, produced by Streptomyces Sp. *Tetrahedron Lett,* 27**,** 2475-2478.

STOCKINGER, L. W., EIDE, K. B., DYBVIK, A. I., SLETTA, H., VÅRUM, K. M., EIJSINK, V. G. H., TØNDERVIK, A. & SØRLIE, M. 2015. The effect of the carbohydrate binding module on substrate degradation by the human chitotriosidase. *BBA Prot. Proteom.,* 1854**,** 1494-1501.

STURTEVANT, J. M. 1977. Heat capacity and entropy changes in processes involving proteins. *Proc. Natl. Acad. Sci. U. S. A.,* 74**,** 2236-2240.

TOMME, P., CREAGH, A. L., KILBURN, D. G. & HAYNES, C. A. 1996. Interaction of polysaccharides with the N-terminal cellulose-binding domain of Cellulomonas fimi CenC. 1. Binding specificity and calorimetric analysis. *Biochemistry,* 35**,** 13885-94.

VAN EIJK, M., SCHEIJ, S. S., VAN ROOMEN, C. P. A. A., SPEIJER, D., BOOT, R. G. & AERTS, J. M. F. G. 2007. TLR- and NOD2-dependent regulation of human phagocyte-specific chitotriosidase. *FEBS Lett.,* 581**,** 5389-5395.

VAN AALTEN, D. M. F., KOMANDER, D., SYNSTAD, B., GÅSEIDNES, S., PETER, M. G. & EIJSINK, V. G. H. 2001. Structural insights into the catalytic mechanism of a family 18 exo-chitinase. *Proc. Natl. Acad. Sci. U.S.A.,* 98**,** 8979-8984.

VAN AALTEN, D. M. F., SYNSTAD, B., BRURBERG, M. B., HOUGH, E., RIISE, B. W., EIJSINK, V. G. H. & WIERENGA, R. K. 2000. Structure of a two-domain chitotriosidase from Serratia marcescens at 1.9-angstrom resolution. *Proc. Natl. Acad. Sci. U.S.A,* 97**,** 5842-5847.

VARNAI, A., MAKELA, M. R., DJAJADI, D. T., RAHIKAINEN, J., HATAKKA, A. & VIIKARI, L. 2014. Carbohydrate-Binding Modules of Fungal Cellulases: Occurrence in Nature, Function, and Relevance in Industrial Biomass Conversion. *In:* SARIASLANI, S. & GADD, G. M. (eds.) *Adv. Appli. Microbiol.* San Diego: Elsevier Academic Press Inc.

VARNAI, A., SIIKA-AHO, M. & VIIKARI, L. 2013. Carbohydrate-binding modules (CBMs) revisited: reduced amount of water counterbalances the need for CBMs. *Biotechnol. Biofuels,* 6**,** 30.

VAAJE-KOLSTAD, G., HORN, S. J., SØRLIE, M. & EIJSINK, V. G. H. 2013. The chitinolytic machinery of Serratia marcescens – a model system for enzymatic degradation of recalcitrant polysaccharides. *FEBS J.,* 280**,** 3028-3049.

WATANABE, T., ITO, Y., YAMADA, T., HASHIMOTO, M., SEKINE, S. & TANAKA, H. 1994. The Roles of the C-Terminal Domain and Type-Iii Domains of Chitinase A1 from Bacillus-Circulans Wl-12 in Chitin Degradation. *J.Bacteriol.,* 176**,** 4465-4472.

WESTERENG, B. 2002. *Structure-function studies of a chitinase, aimed at tailoring its substrate and specificity.*, Norwegian Agricultural University.

WILSON, D. B. 2004. Studies of Thermobifida fusca plant cell wall degrading enzymes. *Chem. Rec.,* 4**,** 72-82.

WISEMAN, T., WILLISTON, S., BRANDTS, J. F. & LIN, L. N. 1989. Rapid measurement of binding constants and heats of binding using a new titration calorimeter. *Anal.Biochem.,* 179**,** 131-137.

ZAKARIASSEN, H. & SØRLIE, M. 2007. Heat capacity changes in heme protein-ligand interactions. *Thermochim.Acta,* 464**,** 24-28.

ZHU, Z., ZHENG, T., HOMER, R. J., KIM, Y. K., CHEN, N. Y., COHN, L., HAMID, Q. & ELIAS, J. A. 2004. Acidic mammalian chitinase in asthmatic Th2 inflammation and IL-13 pathway activation. *Science,* 304**,** 1678-1682.

ZOLOTNITSKY, G., COGAN, U., ADIR, N., SOLOMON, V., SHOHAM, G. & SHOHAM, Y. 2004. Mapping glycoside hydrolase substrate subsites by isothermal titration calorimetry. *Proc. Natl. Acad. Sci. U.S.A,* 101**,** 11275-11280.